Position and momentum bases for the monochromatic Maxwell fish-eye and the sphere

2015 J. Phys. A: Math. Theor. 48 195202

(http://iopscience.iop.org/1751-8121/48/19/195202)

IOP Publishing Journal of Physics A: Mathematical and Theoretical
J. Phys. A: Math. Theor. **48** (2015) 195202 (17pp) doi:10.1088/1751-8113/48/19/195202

Position and momentum bases for the monochromatic Maxwell fish-eye and the sphere

Cristina Salto-Alegre and Kurt Bernardo Wolf

Instituto de Ciencias Físicas, Universidad Nacional Autónoma de México, Av. Universidad s/n, Cuernavaca, Morelos 62210, México

E-mail: salto.alegre@gmail.com and bwolf@fis.unam.mx

Received 22 July 2014, revised 27 December 2014
Accepted for publication 30 March 2015
Published 20 April 2015

Abstract

In geometric optics the Maxwell fish-eye is a medium where light rays follow circles, while in scalar wave optics this medium can only 'trap' fields of certain discrete frequencies. In the monochromatic case characterized by a positive integer ℓ, there are $2\ell + 1$ independent fields. We identify two bases of functions: one, known as the Sherman–Volobuyev functions, is characterized as of 'most definite' momenta; the other is new and composed of 'most definite' positions and normal derivatives for the fish-eye scalar wavefields. Their construction uses the stereographic projection of the sphere, and their identification is corroborated in the $\ell \to \infty$ contraction limit to the homogeneous Helmholtz medium.

Keywords: Maxwell fish-eye, function bases on spheres, position and momentum functions, Sherman–Volobuyev functions, algebra and group contraction, Helmholtz medium

(Some figures may appear in colour only in the online journal)

1. Introduction

The Maxwell fish-eye is one of the 'perfect' geometric optical media studied by Luneburg [1, chapter 28]; it is the stereographic projection from free motion on a sphere onto an inhomogeneous optical medium where ray trajectories are circles. In scalar wave optics this correspondence is mantained with an obliquity factor, subject to the restriction that the wavenumbers in the field be in the spectrum of the Hamiltonian operator on the sphere; this is proportional to squared angular momentum, i.e., to the Casimir operator of the Lie algebra that generates rotations. A well-known basis for each eigenvalue subspace is that of spherical harmonics, and thus their projection on the fish-eye medium.

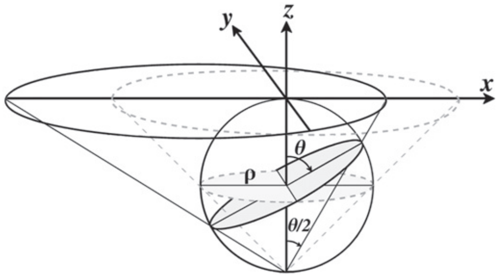

Figure 1. The stereographic map: the top pole of the sphere $\mathcal{S}^2$ of radius ρ is tangent to the optical plane $\mathcal{R}^2$ of the two-dimensional Maxwell fish-eye medium. Free motion on the sphere maps onto motion in circles in the fish-eye (continuous lines). The equator of the sphere maps onto a 'minimal circle' centered on the origin of the fish-eye plane and of least radius 2ρ (dashed lines). A point with colatitude angle θ on the sphere subtends an angle $\frac{1}{2}\theta$ from the bottom pole and maps on the point $x = 2\rho \tan \frac{1}{2}\theta$ in the fish-eye.

The contraction limit of the sphere to the plane yields the homogenous, monochromatic optical Helmholtz medium. In this limit medium one has the well-known basis of plane waves and a basis of Bessel functions on an appropriate set of points, the latter being the best-localized wavefields and normal derivatives in that medium [2]. Understood as bases of 'momenta' and 'positions', the two are related by the wave transform—essentially a projected Fourier transform. In this paper we find the pre-contraction of these two bases on the sphere, and thus on the fish-eye. The 'momentum' wavefunctions on the sphere are related to the Sherman–Volobuyev functions [3, 4]; these are a set of extreme spherical harmonics $Y_{\ell,\ell}$, rotated so that their oscillation belts lie along meridians. The corresponding pre-contracted 'position' wavefunctions on the sphere turn out to be a set of rotated 'mid'-spherical harmonics, $Y_{\ell,0}$ and $Y_{\ell,1} + Y_{\ell,-1}$. The latter we set forth as a basis of best-localized 'position' and 'normal derivative' functions on the sphere, as well as on its projected fish-eye.

The N-dimensional Maxwell fish-eye is 'perfect' because it has a higher symmetry group $\mathsf{SO}(N + 1)$ as shown by Buchdahl [5], within a higher hidden symmetry $\mathsf{SO}(N + 1, 2)$ [6] that is conformal and canonical [7, chapter 6]. It can be thus related to the Kepler and Bohr systems that exhibit the same symmetry [8, 9]; it has supersymmetric features [10], and its various versions also describe classical and quantum systems with position-dependent masses [11–13]. The bases of momentum and position introduced here can be plausibly corresponded with similar ones in those systems.

We work with two-dimensional media for graphical convenience, with the stereographic projection shown in figure 1 that is detailed in section 2. This also describes waveguides with the fish-eye refractive index profile; three- and higher-dimensional versions require hyperspherical harmonics but without further essential changes. Section 3 collects the transformations and limits of the orthonormal basis of spherical harmonics that are needed below. The normalized and adapted Sherman–Volobuyev basis is given in section 4, while what we termed Legendre bases of 'positions and normal derivatives' are developed in section 5. Neither basis is orthogonal though, so wavefields expressed in these bases will present non-local inner products for their expansion coefficients. In section 6 we perform the contraction to the homogeneous Helmholtz medium and verify that the limit yields the bases and unique Euclidean-invariant inner products determined in [2, 14, 15]. Finally, in section 7 we gather some conclusions and perspectives on the use of function bases (rather than eigen-function bases) to obtain a working definition of phase space for the sphere and fish-eye, which are systems whose wavefields live in *finite*-dimensional Hilbert spaces.

2. The stereographic projection

The two-dimensional sphere $\mathcal{S}^2$, in an ambient space of three dimensions, is projected on the two-dimensional optical medium $\mathcal{R}^2$ of the Maxwell fish-eye [16], as shown in figure 1. Points of the sphere $\Omega \equiv (\theta, \phi) \in \mathcal{S}^2$ of radius $\rho > 0$, are mapped on points $\mathbf{r} = (x, y) \equiv r(\cos\phi, \sin\phi) \in \mathcal{R}^2$ of the fish-eye plane, through

$$\tan\frac{1}{2}\theta = r/2\rho, \quad \text{i.e.} \quad \sin\theta = \frac{4\rho r}{4\rho^2 + r^2} \quad \cos\theta = \frac{4\rho^2 - r^2}{4\rho^2 + r^2}, \tag{1}$$

where $r := |\mathbf{r}|$ while $\tan\phi := y/x$ is the same angle in both spaces.

The top pole of the sphere $\theta = 0$ thus maps on the center of the fish-eye $\mathbf{r} = \mathbf{0}$ while the bottom pole $\theta = \pi$ maps to infinity; the equator of the sphere $\theta = \frac{1}{2}\pi$, maps on the minimal circle, which is centered on the origin and has radius $r = 2\rho$. It is shown that on the plane this corresponds to an optical medium of refractive index [1, 5, 16]

$$n(r) = n_o\Big/\Big(1 + r^2\big/4\rho^2\Big), \qquad n_o := (0). \tag{2}$$

Of course, a physical medium is constrained by $n \geqslant 1$, but this is not a mathematical impediment as long as $n > 0$, which allows for all $\mathbf{r} \in \mathcal{R}^2$.

In the geometric-optical model there is a canonically conjugate map in momentum space [7, section 6.4]. This requirement of canonicity is replaced by unitarity in the Hilbert spaces of wave optics. These transformations are reversible and hence conserve the information contained in their respective wavefields.The unitary map of square-integrable functions on the sphere, $F(\Omega) \in \mathcal{L}^2(\mathcal{S}^2)$ onto wavefields $f(\mathbf{r}) \in \mathcal{L}^2(\mathcal{R}^2)$ in the optical plane by (1), determines a relation between the measures on the sphere and the plane

$$\mathrm{d}^2\Omega = \mathrm{d}\cos\theta \; \mathrm{d}\phi = \left(\frac{4\rho}{r^2 + 4\rho^2}\right)^2 r \; \mathrm{d}r \; \mathrm{d}\phi. \tag{3}$$

Functions on the sphere and on the fish-eye must therefore be related with an obliquity weight factor

$$f(\mathbf{r}) = \frac{4\rho}{r^2 + 4\rho^2} F(\Omega(\mathbf{r})), \qquad F(\Omega) = \rho \sec^2\frac{1}{2}\theta \, f(\mathbf{r}(\Omega)). \tag{4}$$

The standard inner product between functions on the sphere integrate over its 4π surface, while wavefields on the fish-eye are integrated over $\mathcal{R}^2$ and bear units of $1/\rho$ due to the obliquity factor. The unitarity of the map (4) determines a Parseval relation between the two function spaces,

$$(F, G)_{\mathcal{S}^2} := \int_{\mathcal{S}^2} \mathrm{d}^2\Omega F(\Omega)^* \, G(\Omega) = \int_{\mathrm{R}^2} \mathrm{d}^2\mathbf{r} f(\mathbf{r})^* \, g(\mathbf{r}) =: (f, g)_{\mathcal{R}^2}. \tag{5}$$

3. Harmonic basis on the sphere

The generators of the Lie algebra $\mathrm{so}(3)$ of rotations are the well-known angular momentum operators $\vec{L} = -\mathrm{i}\vec{s} \times \vec{\nabla}_{\vec{s}}$, $\vec{s} \equiv (x, y, z) \in \mathcal{R}^3$, that obey the commutation relations $[L_i, L_j] = \mathrm{i}L_k$, with i, j, k a cyclic permutation of x, y, z. The self-adjoint irreducible matrix representations of this algebra act on the eigenspaces of the Casimir operator $L^2 = \sum_i L_i^2$

with eigenvalues $\ell(\ell+1)$, and are labeled by the non-negative integer ℓ. The eigenspaces have dimension $2\ell+1$ and spherical harmonics are then classified uniquely as eigenfunctions of L_z, whose spectrum consists of the integer-spaced eigenvalues $m\,|_{-\ell}^{\ell}$.

In the sign convention of Biedenharn and Louck, the spherical harmonics are explicitly given by [17, equations (3.141)–(153)]

$$\begin{aligned} Y_{\ell,m}(\theta,\phi) &= (-1)^m \sqrt{\frac{(2\ell+1)}{4\pi}\frac{(\ell-m)!}{(\ell+m)!}}\; P_\ell^m(\cos\theta)\mathrm{e}^{\mathrm{i}m\phi} \\ &= (-1)^m Y_{\ell,-m}(\theta,-\phi) = (-1)^m Y_{\ell,-m}(\theta,\phi)^*, \end{aligned} \tag{6}$$

where $P_\ell^m(\zeta)$ are the associated Legendre polynomials. They form an orthonormal and complete basis for $\mathcal{L}^2(\mathcal{S}^2)$, namely $(Y_{\ell,m}, Y_{\ell',m'})_{\mathcal{S}^2} = \delta_{\ell,\ell'}\delta_{m,m'}$. For fixed ℓ, and under the same inner product (5), the subset $\{Y_{\ell,m}(\Omega)\}_{m=-\ell}^{\ell}$ forms an orthonormal and complete basis for a $(2\ell+1)$-dimensional space that we indicate by $\mathcal{M}_\ell$. In particular, we shall use below the extreme ($m=\ell$) and the mid ($m=0$) spherical harmonics

$$\begin{aligned} Y_{\ell,\ell}(\theta,\phi) &= \frac{(-1)^\ell}{2^\ell\,\ell!}\sqrt{\frac{(2\ell+1)!}{4\pi}}\,\left(\sin\theta\,\mathrm{e}^{\mathrm{i}\phi}\right)^\ell, \\ Y_{\ell,0}(\theta,\phi) &= \sqrt{\frac{2\ell+1}{4\pi}}\;P_\ell(\cos\theta). \end{aligned} \tag{7}$$

On the fish-eye plane, the wavefields corresponding to the spherical harmonics will be indicated by lower-case letters; according to (1) and (4), they are

$$y_{\ell,m}(\mathbf{r}) = \frac{4\rho}{r^2+4\rho^2}\;Y_{\ell,m}(\Omega(\mathbf{r})). \tag{8}$$

These functions will also be an orthonormal and complete basis for $\mathcal{M}_\ell$ under the inner product (5) that integrates over $\mathcal{R}^2$. In figure 2 we display some of these functions on the sphere and their corresponding projection in the fish-eye plane. We recognize the latter as the monochromatic multipole wavefields.

Azimuthal rotations (around the z-axis), generated by $L_z = -\mathrm{i}\,\partial/\partial\phi$ through $\exp(-\mathrm{i}\alpha L_z)$ multiply the spherical harmonic functions by phases: $Y_{\ell,m}(\theta,\phi-\alpha) = \mathrm{e}^{-\mathrm{i}m\alpha}Y_{\ell,m}(\theta,\phi)$. On the other hand, polar rotations (around the y-axis) yield linear combinations in $\mathcal{M}_\ell$ as

$$\exp\left(-\mathrm{i}\beta L_y\right)Y_{\ell,m}(\theta,\phi) = \sum_{m'=-\ell}^{\ell} Y_{\ell,m'}(\theta,\phi)\,d^{\,\ell}_{m',m}(\beta), \tag{9}$$

where $d^{\,\ell}_{m',m}(\beta)$ are the Wigner *little-d* functions [17, equation (3.72)], explicitly

$$\begin{aligned} d^{\,\ell}_{m',m}(\beta) &= \sqrt{\frac{(\ell+m)!}{(\ell+m')!}\frac{(\ell-m)!}{(\ell-m')!}} \\ &\quad\times\left(\sin\tfrac{1}{2}\beta\right)^{m-m'}\left(\cos\tfrac{1}{2}\beta\right)^{m+m'}\;P_{\ell-m}^{(m-m',m+m')}(\cos\beta) \\ &= d^{\,\ell}_{m,m'}(-\beta) = (-1)^{m-m'}d^{\,\ell}_{m,m'}(\beta) \\ &= (-1)^{m-m'}d^{\,\ell}_{-m',-m}(\beta), \end{aligned} \tag{10}$$

with $P_n^{(\mu,\nu)}(\zeta)$ a Jacobi polynomial.

The $(2\ell+1)\times(2\ell+1)$ matrices $\mathbf{d}^\ell(\beta) := \|d^{\,\ell}_{m,m'}(\beta)\|$ are real, orthogonal, and compose as $\mathbf{d}^\ell(\beta_1)\mathbf{d}^\ell(\beta_2) = \mathbf{d}^\ell(\beta_1+\beta_2)$, $\mathbf{d}^\ell(0) = \mathbf{1}$, and $|d^{\,\ell}_{m,m'}(\beta)| \leqslant 1$. For later use we record the

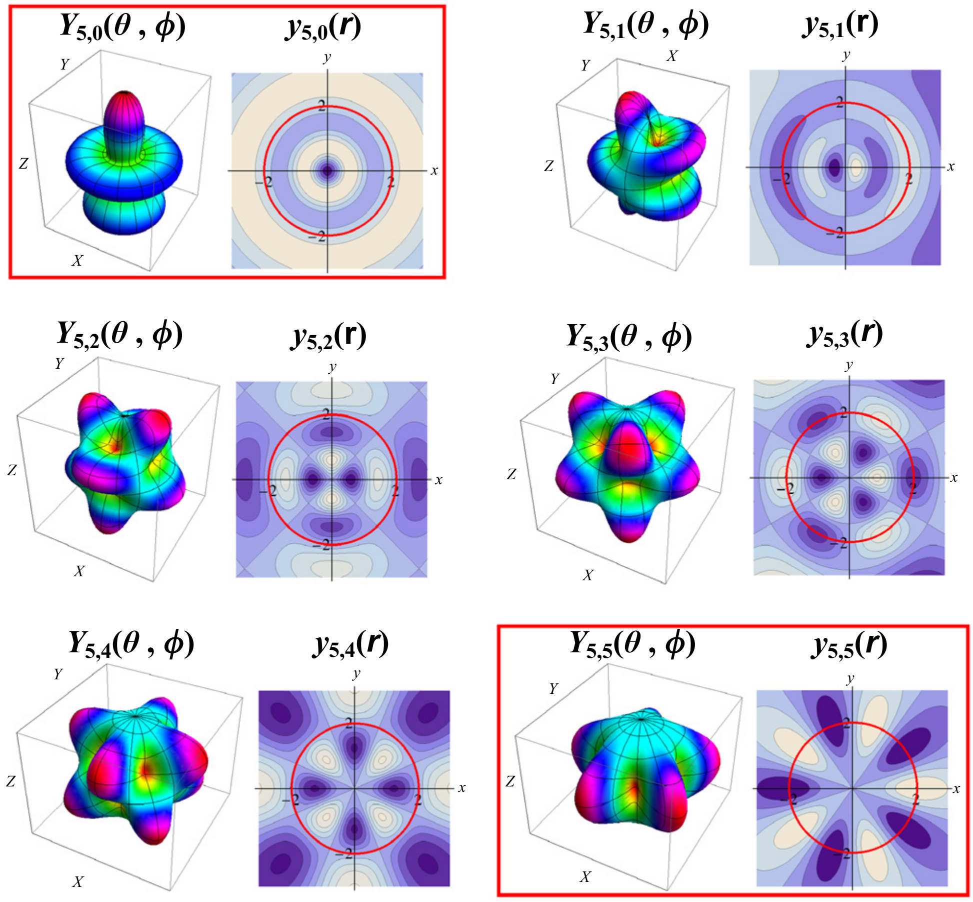

Figure 2. Real part of the spherical harmonics $Y_{5,m}(\theta, \phi)$, $m = 0, 1, \ldots 5$, on the sphere (left of every pair), and $y_{5,m}(\mathbf{r})$ in the fish-eye (right). We mark the 'minimal circle' that projects from the equator of the sphere.

following relations [17, chapter 3]

$$Y_{\ell,m}(\theta, \phi) = \sqrt{\frac{2\ell + 1}{4\pi}}\, d^{\ell}_{m,0}(\theta)\mathrm{e}^{\mathrm{i}m\phi}, \qquad d^{\ell}_{m,\ell}\left(\frac{1}{2}\pi\right) = \frac{1}{2^{\ell}}\sqrt{\binom{2\ell}{\ell + m}}, \tag{11}$$

and the limits

$$\lim_{\rho\to\infty}^{\ell=k\rho} Y_{\ell,m}\left(\frac{r}{\rho}, \phi\right) = (-1)^m\sqrt{\frac{k\rho}{2\pi}}\, J_m(kr)\mathrm{e}^{\mathrm{i}m\phi}, \qquad \lim_{\rho\to\infty}^{\ell=k\rho} d^{\ell}_{m,m'}\left(\frac{r}{\rho}\right) = J_{m-m'}(kr). \tag{12}$$

4. The normalized Sherman–Volobuyev (nShV) basis

The Sherman–Volobuyev functions [3, 4] are proportional to the extreme spherical harmonics $Y_{\ell,\ell}(\theta, \phi)$ in (7), rotated by the polar angle $\beta = \frac{1}{2}\pi$, so that their oscillation belts lie along

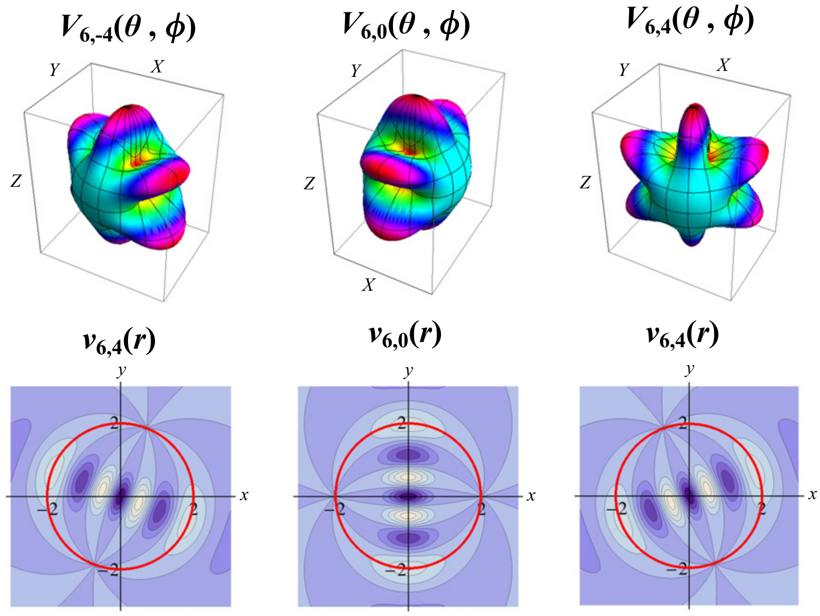

Figure 3. Real part of the normalized Sherman–Volobuyev functions $V_{6,m}(\theta, \phi)$, $m = -4, 0, 4$ in (13) on the sphere (top), and their projections on the fish-eye medium (bottom) with the minimal circle. The full basis is obtained through rotations around the z-axis by $\alpha_m = 2\pi m/(2\ell + 1)$, $m\,|_{-\ell}^{\ell}$.

meridians. They are complete in $\mathcal{L}^2(\mathcal{S}^2)$ for the continuum of azimutal angles $\alpha \in \mathcal{S}^1$. For each ℓ, we can choose $2\ell + 1$ equidistant azimutal angles $\alpha_m := 2\pi m/(2\ell + 1)$, $m\,|_{-\ell}^{\ell}$, to span $\mathcal{M}_\ell$ with the functions

$$\begin{aligned} V_{\ell,m}(\theta, \phi) :=&\ \exp\left(-\mathrm{i}\alpha_m L_z\right)\exp\left(-\mathrm{i}\tfrac{1}{2}\pi L_y\right) Y_{\ell,\ell}(\theta, \phi) \\ =&\ \sum_{m'=-\ell}^{\ell} \exp\left(\frac{-2\pi \mathrm{i} m m'}{2\ell + 1}\right) d^{\ell}_{m',\ell}\left(\tfrac{1}{2}\pi\right) Y_{\ell,m'}(\theta, \phi) \\ =&\ V_{\ell,0}\left(\theta, \phi - \alpha_m\right). \end{aligned} \tag{13}$$

These we call the nShV functions, since they have unit norm under the $\mathcal{L}^2(\mathcal{S}^2)$ inner product. In figure 3 we show some functions $V_{\ell,m}(\theta, \phi)$ over the sphere and their projections on the monochromatic fish-eye medium through (4), that will be indicated by lower-case $v_{\ell,m}(\mathbf{r})$.

The nShV functions have unit norm but are not orthogonal

$$\begin{aligned} \left(V_{\ell,m}, V_{\ell,m'}\right)_{\mathcal{S}^2} &= \left(Y_{\ell,\ell}, \mathrm{e}^{-\mathrm{i}(\alpha_{m'}-\alpha_m)L_y} Y_{\ell,\ell}\right)_{\mathcal{S}^2} \\ &= d^{\ell}_{\ell,\ell}(\alpha_{m'} - \alpha_m) = \left(\cos\frac{\pi(m - m')}{2\ell + 1}\right)^{2\ell}. \end{aligned} \tag{14}$$

No pair of nShV functions $\{V_{\ell,m}(\Omega)\}_{m=-\ell}^{\ell}$ can be orthogonal because in (14), $\frac{1}{2}(\alpha_{m'} - \alpha_m) = \frac{1}{2}\pi$ would imply $m' - m = \ell + \frac{1}{2}$, but all m's are integers. The basis is complete in $\mathcal{M}_\ell$, as one can verify that $\det \| d^{\ell}_{\ell,\ell}(\alpha_{m'} - \alpha_m) \| > 0$. Hence, one can expand any monochromatic function $F(\theta, \phi) \in \mathcal{L}^2(\mathcal{S}^2)$ as

$$F(\theta, \phi) = \sum_{m=-\ell}^{\ell} \widetilde{F}_m \, V_{\ell,m}(\theta, \phi), \tag{15}$$

with generally complex coefficients $\{\widetilde{F}_m\}_{m=-\ell}^{\ell}$. Yet, because this basis of $\mathcal{M}_\ell$ is not orthogonal, the inner product expressed in these coefficients will be nonlocal, i.e., (14) and (15) lead to

$$\begin{aligned}(F, G)_{\mathcal{S}^2} &= \sum_{m,m=-\ell}^{\ell} \widetilde{F}^*_m \big(V_{\ell,m}, V_{\ell,m'} \big)_{\mathcal{S}^2} \widetilde{G}_{m'} \\ &= \sum_{m,m'=-\ell}^{\ell} \widetilde{F}^*_m \left(\cos \frac{\pi(m - m')}{2\ell + 1} \right)^{2\ell} \widetilde{G}_{m'} =: (F, G)_{\mathcal{M}_\ell}.\end{aligned} \tag{16}$$

In section 6 we shall see the $\ell \to \infty$ limit of this inner product of fields contracts to a local inner product of functions over the circle $\alpha \in \mathcal{S}^1$.

5. The Legendre harmonic bases

The 'mid' spherical harmonics $Y_{\ell,0}(\theta, \phi)$ in (7) are real, independent of ϕ, and proportional to the Legendre polynomials $P_\ell(\cos\theta)$. These have two extremal values along the z-axis: a 'finger' of value 1 at $\theta = 0$, and a 'tail' $(-1)^\ell$ at $\theta = \pm\pi$. This axis can be rotated and pointed in any direction of the sphere as shown in figure 4. In the fish-eye medium these functions project on real wavefields with extremal values on two points: the finger on (r, ϕ) and the tail on $(r', \phi + \pi)$, with $rr' = (2\rho)^2$, so the two points are conjugate with respect to the circle of 'minimal radius' projected from the equator $\theta = \frac{1}{2}\pi$, as was noted in section 2. Figure 4 suggests that the mid harmonics are the most localized wavefields; this is borne out by the second moments $\int_{\mathcal{S}^2} \mathrm{d}\Omega \cos^2\theta \, |Y_{\ell,m}(\Omega)|^2$, which are minimal for $m = 0$.

From $Y_{\ell,0}(\theta, \phi) \in \mathcal{L}^2(\mathcal{S}^2)$ we can produce $2\ell + 1$ other functions in $\mathcal{M}_\ell$ by polar rotations through $\beta_m = \pi m/(2\ell + 1)$, $m\,|_{-\ell}^{\ell}$, whose 'fingers' will lie on the upper half-meridian contained in the x–z plane. Since $|\beta_m| < \frac{1}{2}\pi$, all their 'fingers' will lie inside the minimal circle $r = 2\rho$ on the fish-eye plane; while their 'tails' will project on their conjugate points outside. We thus define the Legendre harmonics as

$$\begin{aligned}\Lambda_{\ell,m}(\theta, \phi) :=\ & \mathrm{e}^{-\mathrm{i}\beta_m L_y} Y_{\ell,0}(\theta, \phi) = \sum_{m'=-\ell}^{\ell} d^{\ell}_{m',0}\big(\beta_m\big) Y_{\ell,m'}(\theta, \phi) \\ =\ & d^{\ell}_{0,0}\big(\beta_m\big) Y_{\ell,0}(\theta, \phi) + \sum_{m'=1}^{\ell} d^{\ell}_{m',0}\big(\beta_m\big)\Big(Y_{\ell,m'}(\theta, \phi) + Y_{\ell,m'}(\theta, \phi)^* \Big) \\ =\ & \Lambda_{\ell,m}(\theta, -\phi) = (-1)^\ell \Lambda_{\ell,m}(\theta \pm \pi, \phi),\end{aligned} \tag{17}$$

where we used (6) and (11). On the sphere, all the $\Lambda_{\ell,m}$'s are *even* under $\phi \leftrightarrow -\phi$, and thus their projections on the fish-eye plane under $y \leftrightarrow -y$. They provide therefore a basis only for even functions $F(\theta, \phi) = F(\theta, -\phi)$ in the $(\ell + 1)$-dimensional subspace of $\mathcal{M}_\ell$ spanned by

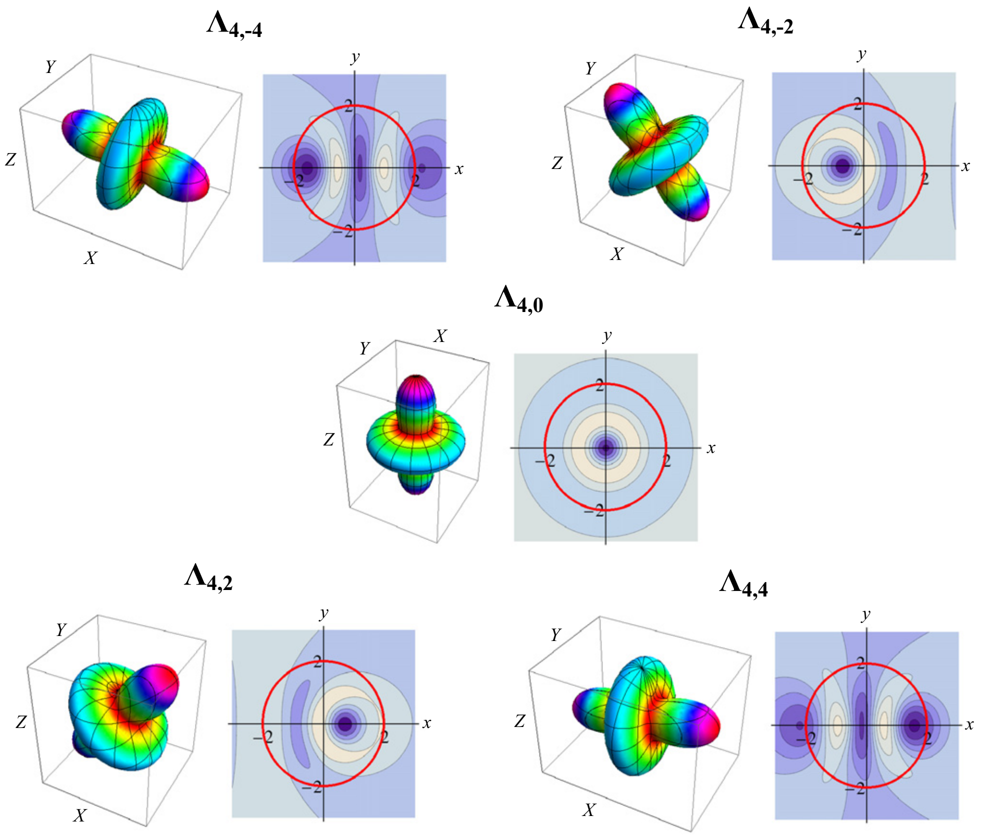

Figure 4. Legendre 'position' functions over the sphere (left of each pair) $\Lambda_{4,m}(\theta, \phi)$, $m = -4, -2, 0, 2, 4$ in (17) which are even in azimuth ϕ; projections on the fish-eye medium (right of each pair) with the minimal circle. The full sub-basis is obtained by y-rotations of $\beta_m = \pi m/(2\ell + 1)$, $m \in \mathcal{E}_\ell$.

Re $Y_{\ell,m}(\theta, \phi) \propto \cos m\phi$. One can verify that the rank of the matrices $\| d^{\ell}_{m,0}(\beta_{m'}) \|$ in (17) is $\ell + 1$, and that the $\Lambda_{\ell,m}$'s in the subset $m \in \mathcal{E}_\ell := \{ -\ell, -\ell + 2, \dots, \ell\}$ are linearly independent, so they can serve as a complete sub-basis for even functions.

We still require a second set of ℓ functions to serve as basis for odd functions $F(\theta, \phi) = -F(\theta, -\phi)$. These can be provided noting from angular momentum theory that

$$\begin{aligned} L_x Y_{\ell,0}(\theta, \phi) &= \tfrac{1}{2}\sqrt{\ell(\ell+1)}\left(Y_{\ell,1}(\theta, \phi) + Y_{\ell,-1}(\theta, \phi)\right) \\ &= -\mathrm{i}\sqrt{\frac{2\ell+1}{4\pi}}\, P^1_\ell(\cos\theta)\sin\phi, \end{aligned} \tag{18}$$

where we have used (6). We thus define a second set of ℓ real normalized functions that are odd in azimuth ϕ on the sphere, and in y on the fish-eye plane, by

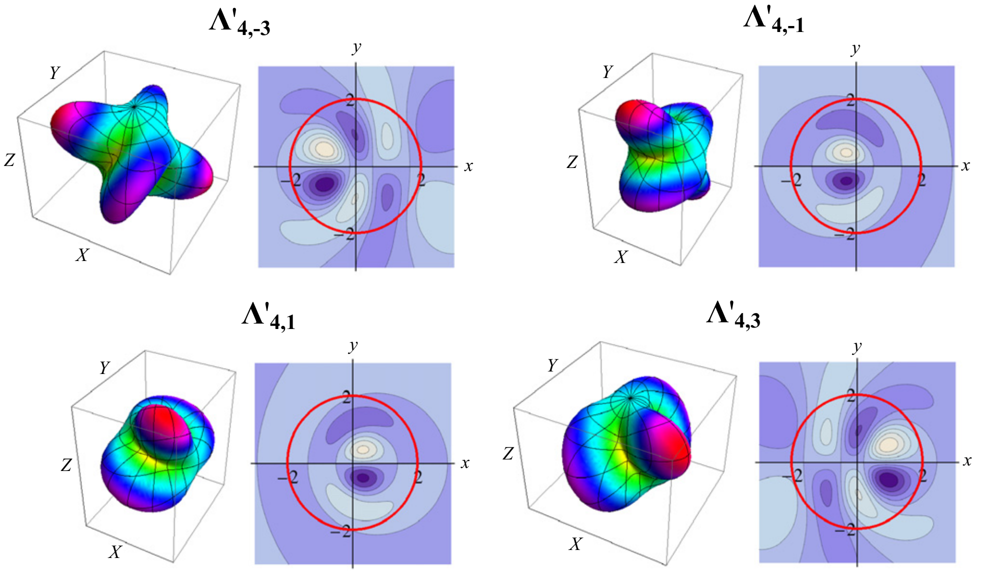

Figure 5. Legendre 'normal derivative' functions over the sphere (left of each pair) $\Lambda'_{4,m}(\theta, \phi)$, $m = -3, -1, 1, 3$ in (19) that are odd in azimuth ϕ; projections on the fish-eye medium (right of each pair) with the minimal circle. The full sub-basis is obtained by y-rotations of $\beta_m = \pi m/(2\ell + 1)$, $m \in \mathcal{E}'_\ell$.

$$\begin{aligned}
\Lambda'_{\ell,m}(\theta, \phi) &:= \sqrt{\frac{2}{\ell(\ell+1)}}\, \mathrm{e}^{-\mathrm{i}\beta_m L_y}(-\mathrm{i})L_x\, \Lambda_{\ell,0}(\theta, \phi) \\
&= \frac{-\mathrm{i}}{\sqrt{2}}\, \mathrm{e}^{-\mathrm{i}\beta_m L_y}\Big(Y_{\ell,1}(\theta, \phi) + Y_{\ell,-1}(\theta, \phi)\Big) \\
&= \frac{-\mathrm{i}}{\sqrt{2}} \sum_{m'=-\ell}^{\ell} \Big(d^{\ell}_{m',1}\big(\beta_m\big) + d^{\ell}_{m',-1}\big(\beta_m\big)\Big) Y_{\ell,m'}(\theta, \phi) \\
&= \frac{-\mathrm{i}}{\sqrt{2}} \sum_{m'=1}^{\ell} \Big(d^{\ell}_{m',1}\big(\beta_m\big) + d^{\ell}_{m',-1}\big(\beta_m\big)\Big)\Big(Y_{\ell,m'}(\theta, \phi) - Y_{\ell,m'}(\theta, \phi)^{*}\Big) \\
&= -\Lambda'_{\ell,m}(\theta, -\phi) = (-1)^{\ell}\Lambda'_{\ell,m}(\theta \pm \pi, \phi),
\end{aligned} \tag{19}$$

which are shown in figure 5. Because on the meridian in the $y = 0$ plane the functions (19) have zero values and maximal derivatives, we call them normal derivative Legendre functions. The subset of $\Lambda'_{\ell,m}$'s with $m \in \mathcal{E}'_\ell := \{ -\ell + 1, -\ell + 3, \ldots, \ell - 1\}$ generate the ℓ-dimensional subspace of $\mathcal{M}_\ell$ functions that are odd in azimuth $\propto \sin m'\phi$. They are linearly independent and form a complete basis for the subspace.

The $\ell + 1$ 'position' functions (17), together with the ℓ 'normal derivative' functions (19), provide us with a proper basis of $2\ell + 1$ independent, real and normalized vectors on the sphere, and hence on the fish-eye medium, for the space of monochromatic functions in $\mathcal{M}_\ell$. The locations of the rotated $+z'$ axes on the sphere and on the fish-eye plane that characterize both the nShV and the Legendre bases are shown in figure 6. There, the points of the nShV functions fall on the equatorial and the minimal circle, as do their conjugate points. The two Legendre sub-bases correspond to alternate points on the upper meridian on the sphere, and on the x-axis of the fish-eye plane inside the minimal circle.

Turning our attention now to the inner products between the functions in the two Legendre sub-bases, we note firstly that $(\Lambda_{\ell,m}, \Lambda'_{\ell,m'})_{S^2} = 0$ due to parity; but neither subset of functions is orthogonal. For the 'position' functions $\Lambda_{\ell,m}$, their inner products are

$$\begin{aligned}\left(\Lambda_{\ell,m}, \Lambda_{\ell,m'}\right)_{S^2} &= \left(Y_{\ell,0}, \mathrm{e}^{-\mathrm{i}\left(\beta_{m'}-\beta_m\right)L_y} Y_{\ell,0}\right)_{S^2}\\ &= d^{\ell}_{0,0}\left(\beta_{m'} - \beta_m\right) = P_\ell\left(\cos\left(\beta_{m'} - \beta_m\right)\right),\end{aligned} \tag{20}$$

where we recall that the Legendre polynomial $P_\ell(\cos\beta)$ contains powers ν of $\cos\beta$, $\nu \in \{\ell, \ell-2, \ldots, 1 \text{ or } 0\}$, or equivalently a linear combination of $\cos\nu\beta$ for the same range of ν. Equation (20) is valid for $m, m'|^{\ell}_{-\ell}$, but is needed only for $m, m' \in \mathcal{E}_\ell$,

The 'normal derivative' functions $\Lambda'_{\ell,m}$ exhibit the inner products

$$\begin{aligned}\left(\Lambda'_{\ell,m}, \Lambda'_{\ell,m'}\right)_{S^2} &= \tfrac{1}{2}\left(\mathrm{e}^{-\mathrm{i}\beta_m L_y}\left(Y_{\ell,1} + Y_{\ell,-1}\right), \mathrm{e}^{-\mathrm{i}\beta_{m'} L_y}\left(Y_{\ell,1} + Y_{\ell,-1}\right)\right)_{S^2}\\ &= d^{\ell}_{1,1}\left(\beta_{m'} - \beta_m\right) + d^{\ell}_{1,-1}\left(\beta_{m'} - \beta_m\right)\\ &= \frac{1}{\ell} P^{(1,1)}_{\ell-1}\left(\cos\left(\beta_{m'} - \beta_m\right)\right) =: Q_{\ell-1}\left(\cos\left(\beta_{m'} - \beta_m\right)\right).\end{aligned} \tag{21}$$

The polynomial $Q_{\ell-1}(\cos\beta)$ is of degree ν in $\cos\beta$, or equivalently a sum of terms $\cos\nu\beta$, where $\nu \in \{\ell-1, \ell-3, \ldots, 0 \text{ or } 1\}$. As before (21), is valid for $m, m'|^{\ell}_{-\ell}$ but is needed only for $m, m' \in \mathcal{E}'_\ell$.

Non-orthogonal bases again involve non-local measures for the expansion coefficients in $\mathcal{M}_\ell$, as was the case for the nShV basis in (16). Functions on the sphere that are linear combinations of both even and odd parts

$$F(\theta, \phi) = \sum_{m\in\mathcal{E}_\ell} F_m \Lambda_{\ell,m}(\theta, \phi) + \sum_{m\in\mathcal{E}'_\ell} F'_m \Lambda'_{\ell,m}(\theta, \phi), \tag{22}$$

will exhibit nonlocal inner products determined by (20) and (21) to be

$$\begin{aligned}(F, G)_{S^2} &= \sum_{m,m'\in\mathcal{E}_\ell} F^*_m\, P_\ell\left(\cos\frac{\pi(m-m')}{2\ell+1}\right) G_{m'} + \sum_{m,m'\in\mathcal{E}'_\ell} F'^*_m\, Q_{\ell-1}\left(\cos\frac{\pi(m-m')}{2\ell+1}\right) G'_{m'}\\ &=: (F, G)_{\mathcal{M}_\ell}.\end{aligned} \tag{23}$$

In the following section we will let $\ell \to \infty$ and contract the 'momentum' and 'position' bases, and their inner products, to those of the homogeneous Helmholtz medium, regaining the known bases and their inner products [2].

6. Contraction of the fish-eye to the homogeneous Helmholtz medium

The Lie algebra so(3) of rotations that served to characterize the function bases on the sphere and the projected wavefields on the two-dimensional fish-eye medium, can be contracted to the Euclidean Lie algebra iso(2) that generates rotations and translations on the plane [18]. We apply this contraction to the spherical harmonics and to the new bases that we built in the last two sections.

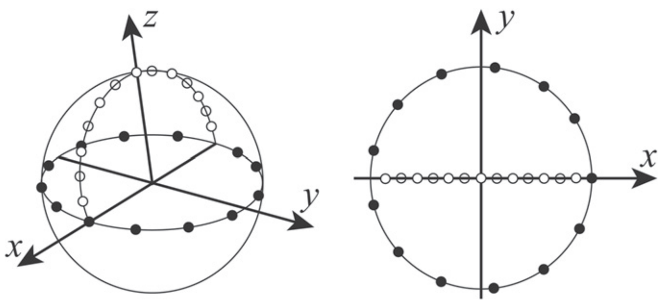

Figure 6. *Left*: the rotated $+z$ axes of the nShV basis of 'momentum' functions $V_{\ell,m}$ over the sphere (marked •) lie around the equator; those of the Legendre 'position' and 'normal derivative' functions $\Lambda_{\ell,m}$ (O) and $\Lambda'_{\ell,m}$ (⊖), are in the upper half-meridian in the $y = 0$ plane. *Right*: their stereographic projections on the fish-eye plane for the nShV basis are points on the minimal circle, while for the two Legendre sub-bases are alternating points on the x-axis inside the minimal circle .

6.1. The contraction parameter and the wavenumber

When the radius ρ of the sphere in figure 1 grows without bound, its symmetry group contracts from $\mathsf{so}(3)$ to $\mathsf{iso}(2)$. In the limit $\rho \to \infty$ the refractive index (2) becomes constant, $n(\mathbf{r}) = n_o$, so the Maxwell fish-eye becomes a homogeneous medium where we should ask its wavefields to retain a definite wavenumber. Only a correspondingly growing representation index $\ell \propto \rho$ will prevent the projected wavefields from becoming constant. The nShV functions should retain the same wavelength λ on the sphere where it is tangent to the fish-eye plane. Since $2\pi\rho$ is the perimeter of any maximal circle, $Y_{\ell,\ell}(\theta, \phi) \propto \exp\, \mathrm{i}\ell\phi$ will accommodate around it ℓ wavelengths $\lambda = 2\pi\rho/\ell$. The contraction $\mathsf{so}(3) \to \mathsf{iso}(2)$ when $\rho, \ell \to \infty$ will thus be determined by the ratio

$$k = \ell/\rho = 2\pi/\lambda, \quad \ell = k\rho, \tag{24}$$

which is the wavenumber of the wavefield in the homogeneous medium n_o. The polar angle θ in the growing sphere will map onto a finite radius r on the fish-eye plane (1) when

$$\sin\theta = 4\rho r/\left(4\rho^2 + r^2\right) \quad \to \quad \theta \approx r/\rho. \tag{25}$$

The limit $\rho \to \infty$ of the fish-eye spherical harmonic basis, $\{y_{\ell,m}(\mathbf{r})\}_{m=-\ell}^{\ell}$ in (8), is given by (12). The dependence on $\sqrt{\rho}$ is eliminated renormalizing by $1/\sqrt{\rho}$ the functions under contraction. One then obtains the Bessel-multipole basis of wavefields

$$\begin{aligned} \mu_m(\mathbf{r}) &:= \lim_{\substack{\ell=k\rho \\ \rho\to\infty}} \frac{1}{\sqrt{\rho}} y_{\ell,m}(\mathbf{r}) \\ &= (-1)^m \sqrt{\frac{k}{2\pi}} J_m(kr) \mathrm{e}^{\mathrm{i}m\phi}, \qquad m\,|_{-\infty}^{\infty}, \end{aligned} \tag{26}$$

that form a well-known denumerable basis for the space of (non-exponential) solutions in a Helmholtz medium.

Under the contraction, rotations around the z-axis of the sphere remain as rotations of the x–y fish-eye plane around its center. On the other hand rotations around the x- and y- axes, since $z \approx \rho \to \infty$, become translations in the y- and x-directions of the fish-eye plane, generated by

$$L_x = -\mathrm{i}\left(y\partial_z - z\partial_y\right) \to \mathrm{i}\rho\partial_y,$$
$$L_y = -\mathrm{i}\left(z\partial_x - x\partial_z\right) \to -\mathrm{i}\rho\partial_x, \tag{27}$$

and the finite displacement operators become $\mathrm{e}^{-\mathrm{i}\beta_m L_y} \to \mathrm{e}^{-x_m\partial_x}$, for finite $x_m \approx \beta_m\rho$, so $\beta \propto 1/\rho$. The limit of the Casimir operator is $L^2 = \ell(\ell+1)1 \to \rho^2(\partial_x^2 + \partial_y^2) = \rho^2 k^2 1$; factoring out ρ^2, this determines the Helmholtz equation for fields of wavenumber k.

6.2. Contraction of the nShV basis

As the dimension of the space $\mathcal{M}_\ell$ of fish-eye monochromatic wavefields increases, the azimuth angles of the members of the nShV basis, $\alpha_m = 2\pi m/(2\ell+1)$, $m\,|_{-\ell}^{\ell}$, as defined in (13), become dense on the α-circle, separated by a vanishing $\Delta\alpha = 2\pi/(2\ell+1) \to 0$. Hence $\alpha \equiv \alpha_m$ on the circle will take the place of m as a label for the limit fields.

It is to be expected that the nShV functions $V_{\ell,m}(\theta, \phi)$ will contract to plane waves; indeed, the ρ, $\ell \to \infty$ limit (24) and (25) of the nShV basis (13) is given by the growing sum

$$V_{\ell,m}(r/\rho, \phi) = \sum_{m'=-\ell}^{\ell} \mathrm{e}^{-\mathrm{i}m'\alpha_m} d^{\,\ell}_{m',\ell}\left(\frac{1}{2}\pi\right) Y_{\ell,m'}(r/\rho, \phi), \tag{28}$$

$$\to \sum_{m'=-\infty}^{\infty} (-1)_{m'} \frac{\mathrm{e}^{-\mathrm{i}m'\alpha_m}}{(\pi\ell)^{1/4}} \sqrt{\frac{k\rho}{2\pi}}\, J_{m'}(kr)\mathrm{e}^{\mathrm{i}m'\phi}, \tag{29}$$

$$= \frac{1}{\sqrt{2\pi}}\left(\frac{k\rho}{\pi}\right)^{1/4} \sum_{m'=-\infty}^{\infty} \mathrm{e}^{\mathrm{i}m'(\phi-\alpha+\pi)} J_{m'}(kr). \tag{30}$$

In (29) we used (11) for $\lim_{\ell\to\infty} d^{\,\ell}_{m',\ell}(\frac{1}{2}\pi) = (\pi\ell)^{-1/4}$, which is valid when $|m'| \ll \ell$, while for the $Y_{\ell,m'}$'s we used (12), noting that since the Bessel functions $J_{m'}(kr)$ have m'-fold zeros at $r = 0$ and are small for $kr < m'$, large m''s will yield vanishing contributions to finite regions of the fish-eye plane. We thus write the Helmholtz wavefields renormalizing by $\rho^{-1/4}$ and use the Bessel generating function to obtain

$$v_{k,\alpha}(r, \phi) := \lim_{\rho\to\infty}^{\ell=k\rho} \rho^{-1/4} V_{\ell,m}(r/\rho, \phi)$$
$$= \frac{(k/\pi)^{1/4}}{\sqrt{2\pi}} \exp(\mathrm{i}kr\sin(\phi-\alpha)). \tag{31}$$

These are plane waves of wavenumber k whose wavefronts lie in the $\phi = \alpha$ direction. Another look at equation (30) reveals the expansion of plane waves into multipole wavefields (26).

The expansion of a generic Helmholtz wavefield $f(\mathbf{r})$ in terms of the circle of plane waves (31) is the limit of (15) when $\rho \to \infty$; the sum over α_m, $m\,|_{-\ell}^{\ell}$, with $\Delta\alpha = 2\pi/(2\ell+1) \to 0$ becomes a Riemann integral over the α-circle in the same way that finite Fourier transforms limit to Fourier series on the circle, i.e.

$$f(\mathbf{r}) = \frac{1}{\Delta\alpha}\sum_{m=-\ell}^{\ell} \Delta\alpha\, \widetilde{f}_m\, v_{\ell,m}(\mathbf{r}) \to \int_{-\pi}^{\pi} \mathrm{d}\alpha\, \widetilde{f}(\alpha)\, \mathrm{e}^{\mathrm{i}kr\sin(\phi-\alpha)}. \tag{32}$$

The inner product between two functions F, G on the sphere in (16) entailed, for finite ρ, a non-local inner product between their coefficients $\widetilde{F}_m$, $\widetilde{G}_{m'}$. In the ρ, $\ell \to \infty$ limit, this non-local kernel becomes a Dirac δ

$$\lim_{\rho\to\infty}^{\ell=k\rho}\left(\cos\frac{\pi(m-m')}{2\ell+1}\right)^{2\ell}=\frac{1}{\sqrt{\pi k\rho}}\delta(\alpha-\alpha'),\tag{33}$$

so the inner product of two Helmholtz wavefields f, g in terms of the coefficient functions $\widetilde{f}(\alpha)$, $\widetilde{g}(\alpha)$ in (32), becomes *local*:

$$(f, g)_\circ := \int_{-\pi}^{\pi} \mathrm{d}\alpha \widetilde{f}(\alpha)^* \widetilde{g}(\alpha).\tag{34}$$

To prove (33), note that for $m \neq m'$, $\cos(\alpha_m - \alpha_{m'}) < 1$, so its growing powers tend to zero; on the other hand the sum → integral of $\alpha_m \to \alpha$ in (33) is asymptotically $1/\sqrt{(\pi\ell)}$ [19, equation (3.621.3)]. The powers the two factors of $\rho^{1/4}$ in the renormalized functions (30) and the factor of $\rho^{-1/2}$ in (33) cancel.

The basis of plane waves, $\{v_{k,\alpha}(\mathbf{r})\}_{\alpha\in S^1}$ in (31), is the basis of Euclidean momentum in the Helmholtz medium [14]; its pre-contraction, the nShV basis on the sphere $\{V_{\ell,m}(\theta, \phi)\}_{m=-\ell}^{\ell}$ in (13), can be seen as the natural momentum basis on the sphere, as was understood by Sherman and Volobuyev [3, 4], and its projection in the monochromatic Maxwell fish-eye as well.

6.3. Contraction in the legendre basis

The two Legendre sub-bases, $\Lambda_{\ell,m}(\theta, \phi)$ and $\Lambda'_{\ell,m}(\theta, \phi)$ in (17) and (19), point their 'fingers' at angles $\beta_m = \pi m/(2\ell + 1)$, and project these maxima on points x_m on the x-axis of the fish-eye plane. As we saw, for $m \in \mathcal{E}_\ell$, the former are the $\mathcal{M}_\ell$ sub-basis of even functions, and for $m \in \mathcal{E}'_\ell$ of odd functions, in azimuth $\phi \leftrightarrow -\phi$, and in $y \leftrightarrow -y$ on the fish-eye plane.

In the ℓ, $\rho \to \infty$ limit (24), the set of points x_m, $m \in \mathcal{E}_\ell$ or $\mathcal{E}'_\ell$, will project on the infinite set of equally-spaced points

$$x_m = 2\rho \tan\frac{1}{2}\beta_m \quad\to\quad x_m = \rho\beta_m = \frac{1}{4}\lambda m.\tag{35}$$

The contraction of the position Legendre basis can be found by considering first $\Lambda_{\ell,0}$, i.e. $\beta_0 = 0$, whose Legendre 'finger' points at the origin of the fish-eye $\mathbf{r}$-plane, $x_0 = 0$. There, $d^{\ell}_{m',0}(0) = \delta_{m',0}$ reduces the sum in (17) to a single term $Y_{\ell,0}(\theta, \phi)$, where we use (12) for finite $r = \rho\theta$. Its limit is

$$\lim_{\rho\to\infty}^{\ell=k\rho}\Lambda_{\ell,0}(r/\rho, \phi) = \sqrt{\frac{k\rho}{2\pi}}J_0(kr).\tag{36}$$

Since rotations around the y-axis have contracted to translations in the x direction, all other $\Lambda_{\ell,m}$'s will be x_m-translated versions of (36) for $m \in \mathcal{E}_\ell$. These points are equidistant by half-wavelengths $\frac{1}{2}\lambda$, each the center of a displaced monopole field.

On the Helmholtz plane, and renormalized by $1/\sqrt{\rho}$, the contraction limit of the Legendre position functions is

$$\lambda_{k,m}(\mathbf{r}) := \lim_{\rho\to\infty}^{\ell=k\rho}\frac{1}{\sqrt{\rho}}\Lambda_{\ell,m}(r/\rho, \phi) = \sqrt{\frac{k}{2\pi}}\, J_0\big(k|\mathbf{r}-\mathbf{x}_m|\big),\tag{37}$$

where $|\mathbf{r} - \mathbf{x}_m| = \sqrt{[(x - x_m)^2 + y^2]}$ and $kx_m = \frac{1}{4}\pi m$, for all even $m \in \mathcal{E}_{\text{even}}$. Since the J_0's in (37) are known to be the narrowest Helmholtz wavefields [2], with the role of position

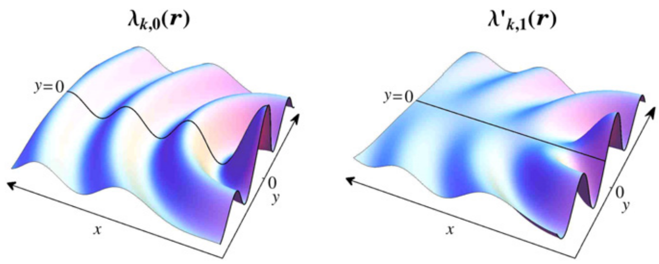

Figure 7. *Left*: the limit of the Legendre 'position' functions are the J_0-Bessel functions $\lambda_{k,m}(\mathbf{r})$ in (37) centered on x_m, $m \in \mathcal{E}_{\text{even}}$. *Right*: the limit of the 'normal derivative' Legendre functions $\lambda'_{k,m}(\mathbf{r})$ in (39), which are centered on x_m, $m \in \mathcal{E}_{\text{odd}}$.

functions forming a basis for fields $f(x, y)$ that are even in $y \leftrightarrow -y$. This identification thus extends back to the Legendre basis on the pre-contracted sphere.

The $\ell, \rho \to \infty$ limit of the normal derivative functions, $\Lambda'_{\ell,m}(\theta, \phi)$ in (19), when $\rho \to \infty$, $\theta = r/\rho \to 0$ and $\beta_m = x_m/\rho \to 0$, can be found with the y-derivative of (27) on (36) as function of $\mathbf{r} = (x, y)$, namely

$$\lim_{\rho\to\infty}^{\ell=k\rho} \Lambda'_{\ell,m}(\theta, \phi) = \mathrm{i}\sqrt{\frac{\rho}{\pi k}}\, \mathrm{e}^{-x_m \partial_x} \frac{\partial}{\partial y} J_0(kr) = \mathrm{i}\sqrt{\frac{\rho k}{\pi}} \frac{J_1\big(k|\mathbf{r} - \mathbf{x}_m|\big)}{|\mathbf{r} - \mathbf{x}_m|} y. \tag{38}$$

We thus complement the set of functions (37) with

$$\lambda'_{k,m}(\mathbf{r}) := \lim_{\rho\to\infty}^{\ell=k\rho} \frac{-\mathrm{i}}{\sqrt{\rho}} \Lambda'_{\ell,m}(\theta, \phi) = \sqrt{\frac{k}{\pi}} \frac{J_1\big(k|\mathbf{r} - \mathbf{x}_m|\big)}{|\mathbf{r} - \mathbf{x}_m|} y, \tag{39}$$

for $kx_m = \frac{1}{4}\pi m$, for all odd $m \in \mathcal{E}_{\text{odd}}$. We note that $y/|\mathbf{r} - \mathbf{x}_m| = \sin \phi_m$, where ϕ_m is the polar angle in the plane referred to the point $\mathbf{x}_m$. The Helmholtz limit wavefunctions (37) and (39) are shown in figure 7 for $m = 0$; all others are only x-translated versions of these two for $m \in \mathcal{E}_{\text{even}}$ or $\mathcal{E}_{\text{odd}}$.

Generic Helmholtz wavefields can be written in terms of the position and normal derivative bases (37) and (39) as

$$f(\mathbf{r}) = \sum_{m\in\mathcal{E}_{\text{even}}} f_m\, \lambda_{k,m}(\mathbf{r}) + \sum_{m\in\mathcal{E}_{\text{odd}}} f'_m\, \lambda'_{k,m}(\mathbf{r}). \tag{40}$$

The inner product between two of these fields f, g, given in terms of their coefficients f_m, f'_m, $g_{m'}$, $g'_{m'}$, is the limit of the finite case whose non-local inner product was (23). Now, using (12) and

$$\begin{aligned} \lim_{\rho\to\infty}^{\ell=k\rho} \Big(d^{\,\ell}_{m,1}(x/\rho) + d^{\,\ell}_{m,-1}(x/\rho)\Big) &= J_{m-1}(kx) + J_{m+1}(kx) \\ &= \frac{2m}{kx} J_m(kx), \end{aligned} \tag{41}$$

for $m = 1$, we find that the inner product remains non-local in the coefficients at the discrete positions x_m

$$(f,\, g)_{\mathcal{Z}} := \sum_{m,m'\in\mathcal{E}_{\rm even}} f_m^*\, J_0\!\left(\frac{1}{2}\pi(m'-m)\right) g_{m'} + \sum_{m,m'\in\mathcal{E}_{\rm odd}} f_m'^{\,*}\, \frac{J_1\!\left(\frac{1}{2}\pi(m'-m)\right)}{\frac{1}{2}\pi(m'-m)}\, g'_{m'}. \qquad (42)$$

This can be compared with the same nonlocal inner product that appears in [2, 14, 15]; it was built in [14] and shown to be the only $\mathsf{iso}(2)$-invariant sesquilinear inner product, i.e., whose 'measurement line' of x_m's can be rotated and translated without changing its value.

7. Conclusions

Beside the natural, orthonormal basis of spherical harmonics for functions on the sphere, $\{Y_{\ell,m}\}_{m=-\ell}^{\ell}$ with fixed ℓ, we determined a normalized finite sub-basis of that introduced by Sherman and Volubuyev [3, 4] to stand for the $2\ell + 1$ states of momentum, which are rotated copies of $Y_{\ell,\ell}$. We also proposed a new basis, associated to the name of Legendre, which is composed of $2\ell + 1$ interdigitated functions of position and normal derivative that are rotated versions of $Y_{\ell,0}$ and of $Y_{\ell,1} + Y_{\ell,-1}$ respectively. Finally, when the sphere contracts to a plane, we matched the limits of these bases with previously known bases for Helmholtz monochromatic wavefields in the appropriate Hilbert space. This is in analogy to other studies of discrete and finite Hamiltonian systems that contract to continuous quadratic quantum systems in the limit when the number and density of points grow without bound [15, 20–23].

There is a fundamental difference though: whereas in those finite systems the bases were determined as eigenfunctions of a set of commuting operators in a Lie algebra, here they were determined through finite elements of a group acting on the above-quoted fiducial functions. Whereas the eigenfunctions form orthogonal bases, the function sets we considered here do not, yet they lie within a definite Hilbert- and group-theoretic structure which contracts to Euclidean and conformal optics [7, appendix B] and which is applicable both to the geometric and scalar wave models.

One area of interest in exploring finite systems that are pre-contracted versions of a continuous one, is to ensure that a succession of finite approximations, harboring the symmetries of the continuous limit, will properly converge to it. Another wide area pertains phase space, which is well understood in classical mechanics and geometric optics, and also in quantum mechanics via the Wigner function associated to the Heisenberg–Weyl group that hardly needs reference; a finite periodic version, the Wigner function on a discrete torus, derives directly from that.

For functions on the sphere, a phase space and Wigner function were defined on the original Sherman–Volobuyev basis in [24]. Moreover, for finite systems associated to the rotation algebra $\mathsf{so}(3)$, a spherical phase space and the corresponding Wigner function were introduced in [25], which may be best applicable here. On the other hand, for continuous Euclidean-invariant systems such as that obeying the Helmholtz equation, several phase spaces and Wigner functions have been analyzed by various authors [26–29], one of which has been shown to be particularly useful for electromagnetic optics [30]. In each of those representations, the bases introduced here as multipole, momentum and Legendre functions, are expected to have definite shape signatures, as coherent states do under the traditional Wigner function, which should take into account the non-locality of their inner products [31]. We leave this subject for further study.

Acknowledgments

We thank Guillermo Krötzsch for comments and his assistance in the preparation of the figures. Support for this research has been provided by the *Óptica Matemática* projects by the Universidad Nacional Autónoma de México (PAPIIT IN101115).

References

[1] Luneburg R K 1964 *Mathematical Theory of Optics* (Berkeley, CA: University of California Press)
[2] González-Casanova P and Wolf K B 1995 Interpolation of solutions to the Helmholtz equation *Numer. Methods Partial Differ. Equ.* **11** 77–91
[3] Sherman T O 1975 Fourier analysis on the sphere *Trans. Am. Math. Soc.* **209** 1–31
[4] Volobuyev I P 1980 Plane waves on the sphere and some of their applications *Teor. Mat. Fiz.* **45** 421–6
[5] Buchdahl H A 1978 Kepler problem and Maxwell fish-eye *Am. J. Phys.* **46** 840–3
[6] Frank A, Leyvraz F and Wolf K B 1990 Hidden symmetry and potential group of the Maxwell fish-eye *J. Math. Phys.* **31** 2757–68
[7] Wolf K B 2004 *Geometric Optics on Phase Space* (Heidelberg: Springer)
[8] Demkov Y N and Ostrovsky V N 1971 Internal symmetry of the Maxwell 'fish-eye' problem and the Fock group for the hydrogen atom *Sov. Phys. JETP* **33** 1083–7
[9] Chen A C 1979 The Coulomb problem and the Maxwell fish-eye problem *Am. J. Phys.* **46** 214–7
[10] Roşu H C *et al* 1996 Supersymmetric features of the Maxwell fish-eye lens *SPIE Proc.* **2730** 436–9
[11] Cruz S, Cruz Y, Negro J and Nieto L M 2007 Classical and quantum position-dependent mass harmonic oscillators *Phys. Lett.* A **369** 400–6
[12] Cruz S, Cruz Y and Rosas-Ortiz O 2009 Position-dependent mass oscillators and coherent states *J. Phys. A: Math. Theor.* **42** 185205
[13] Makowski A J and Górska K J 2009 Quantization of the Maxwell fish-eye problem and the quantum–classical correspondence *Phys. Rev.* A **79** 052116
[14] Steinberg S and Wolf K B 1981 Invariant inner products on spaces of solutions of the Klein–Gordon and Helmholtz equations *J. Math. Phys.* **22** 1660–3
[15] Wolf K B 2013 Continuous versus discrete free Hamiltonian systems *J. Phys. A: Math. Theor.* **46** 335202
[16] Maxwell J C 1854 Solution of a problem *Camb. Dublin Math. J.* **8** 188–93
[17] Biedenharn L C and Louck J D 1981 *Angular Momentum in Quantum Physics, Theory and Application* (*Encyclopedia of Mathematics and Its Applications)* vol 8) ed G-C Rota (Reading, MA: Addison-Wesley)
[18] Gilmore R 1978 *Lie Groups, Lie Algebras, and Some of their Applications* (New York: Wiley Interscience)
[19] Gradshteyn I S and Ryzhik I M 2000 *Tables of Integrals Series and Products* 6th edn (San Diego: Academic)
[20] Atakishiyev N M, Pogosyan G S and Wolf K B 2005 Finite models of the oscillator *Phys. Part. Nuclei* **36** 521–55
[21] Wolf K B 2010 Discrete systems and signals on phase space *Appl. Math. Inf. Sci.* **4** 141–81
[22] Jafarov E I, Stoilova N I and van der Jeugt J 2011 Finite oscillator models: the Hahn oscillator *J. Phys. A: Math. Theor.* **44** 265203
[23] Jafarov E I, Stoilova N I and van der Jeugt J 2011 The su(2) Hahn oscillator and a discrete Fourier–Hahn transform *J. Phys. A: Math. Theor.* **44** 355205
[24] Alonso M A, Pogosyan G S and Wolf K B 2003 Wigner functions for curved spaces: II. On spheres *J. Math. Phys.* **44** 1472–89
[25] Atakishiyev N M, Chumakov S M and Wolf K B 1998 Wigner distribution function for finite systems *J. Math. Phys.* **39** 6247–61
[26] Nieto L M, Atakishiyev N M, Chumakov S M and Wolf K B 1998 Wigner distribution function for Euclidean systems *J. Phys. A: Math. Theor.* **31** 3875–95

[27] Wolf K B, Alonso M A and Forbes G W 1999 Wigner functions for Helmholtz wavefields *J. Opt. Soc. Am.* A **16** 2476–87
[28] Alonso M A 2000 Measurement of Helmholtz wavefields *J. Opt. Soc. Am.* A **17** 1256–64
[29] Alonso M A 2004 Wigner functions for nonparaxial, arbitrarily polarized electromagnetic wave fields in free space *J. Opt. Soc. Am.* A **21** 2233–43
[30] Alonso M A 2001 Radiometry and wide-angle wave fields: I. Coherent fields in two dimensions *J. Opt. Soc. Am.* A **18** 902–9
[31] Ali S T, Atakishiyev N M, Chumakov S M and Wolf K B 2000 The Wigner function for general Lie groups and the wavelet transform *Ann. Henri Poincaré* **1** 685–714